T25B-0172

Constraints on the Mantle Wavespeed and Discontinuity Structure below the Turkana Depression, East Africa: Insights into Topographic Development and Ethiopian Flood Basalt Volcanism

[1*]Alistair Boyce, [2]Rita Kounoudis, [2]Ian D. Bastow, [1]Sanne Cottaar, [3]Cynthia. J. Ebinger, [2]Christopher S. Ogden

[1*]University of Cambridge, [2]Imperial College London, [3]Tulane University, Université Claude Bernard Lyon 1

1 Overview

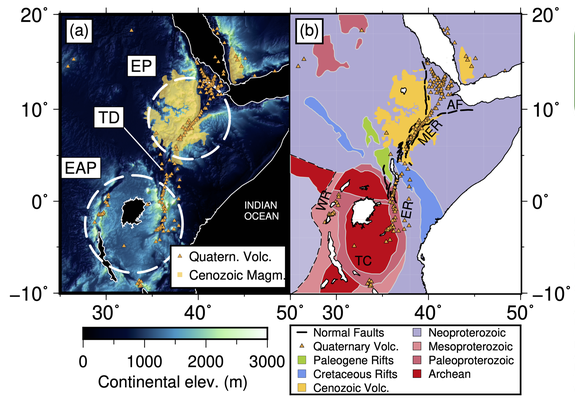

FIGURE 1: (a) The Ethiopian (EP) and East African (EAP) topographic plateaus are separated by the Turkana Depression (TD). Cenozoic flood basalt magmatism and Quaternary volcanism are marked. **(b)** Broad-scale East African tectonics modified after Begg et al., (2009). Normal faults bounding the Neogene-Recent East African rift (black lines). AF: Afar Depression, ER: East African Rift, MER: Main Ethiopian Rift, TC: Tanzanian Craton, WR: Western Rift.

Check this out too!

Pugh et al.,

"The X-discontinuity as a Tracer for Chemical Heterogeneity: Observations from East Africa"

Poster: DI25B-0029

Tuesday 14th Dec. 16:00-18:00

- **Mechanisms to explain the subdued topography of the Turkana Depression that separates the elevated Ethiopian and East African plateaus in East Africa are debated because constraints on upper mantle structure and dynamics are lacking.**
- **Attempts to understand the role of the mantle below Turkana in the evolution of rifting between the MER and Eastern Rifts and the onset of Ethiopian flood basalt volcanism are also hindered by limited data availability.**
- **New data from recently deployed seismic networks in Turkana and neighboring Uganda enable us to address these issues using two approaches.**
- **Building on the work of Boyce et al., (2021), we develop a new absolute P-wavespeed tomographic model (AFRP21) to image mantle structure below the Turkana Depression.**
- **We also supplement the P-to-s receiver function database of Boyce & Cottaar (2021) with the newly available data to map the mantle transition zone (MTZ) discontinuity structure below Turkana.**

4 Receiver Function Data and Methods

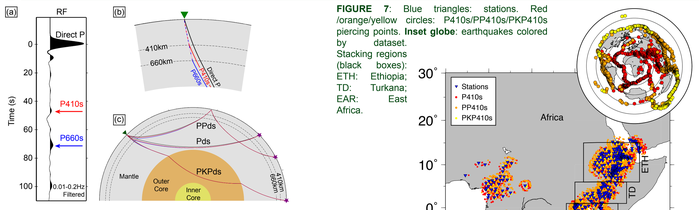

FIGURE 6: **(a)** Example Pds phase receiver function (RF). Low amplitude P-to-s converted phases from top and bottom of the MTZ are indicated. **(b)** Ray path diagram showing incoming converted P (solid) to s (dashed) phases at MTZ discontinuities w.r.t. direct P phase. **(c)** Converted and direct phases take largely similar paths throughout Earth's mantle. Adapted after Jenkins et al., (2016).

FIGURE 7: Blue triangles: stations. Red /orange/yellow circles: P410s/PP410s/PKP410s piercing points. **Inset globe**: earthquakes colored by dataset. Stacking regions (black boxes): ETH: Ethiopia; TD: Turkana; EAR: East Africa.

- Receiver functions (RFs) calculated using time-domain iterative deconvolution (Ligorria & Ammon,1999) are built with 5s width Gaussian pulses (Fig. 6).
- Boyce & Cottaar (2021) data set supplemented by waveform data from the Turkana Depression and neighboring Uganda (Fig. 7).
- Final high quality Pds, PPds, PKPds data set restricted to 40-90°, 100-125°, 145-150° epicentral distance respectively (Fig. 8) following strict QC.

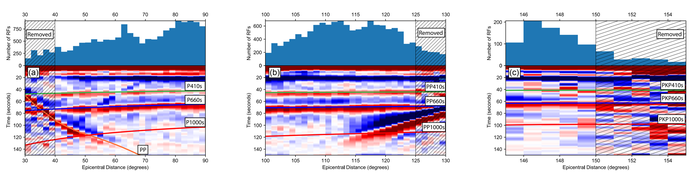

FIGURE 8 (Below): RFs (filtered at 0.01-0.2Hz) binned by epicentral distance for 16,701 Pds RFs **(a)**, 13,865 PPds RFs **(b)** and 899 PKPds RFs **(c)**. Predicted moveout of converted phases are labelled. "Removed" epicentral distance bins are excluded from subsequent CCP stacking to limit interference of multiples with MTZ converted arrivals.

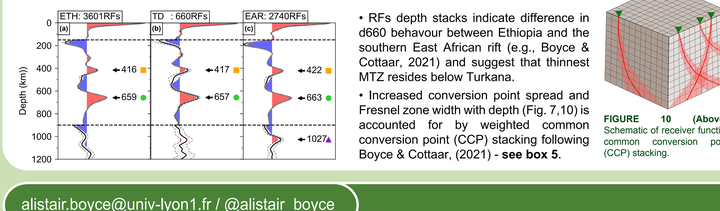

FIGURE 9 (Below): Regional depth stacks for Pds data whose piercing points at 410km depth fall within regions ETH **(a)**, TD **(b)**, EAR **(c - see Fig. 7)**. RF max frequency is 0.2Hz. Depth stacks comprise RFs corrected to depth using the AF2019 tomographic model (Celli et al., 2020) within which the depths of high amplitude positive peaks are labeled. Below 150 km and 900 km, depth stack amplitudes are multiplied by five and twenty respectively. Orange square: d410 conversion/multiple. Green circle: d660 conversion/multiple. Violet triangle: d1000 conversion/multiple.

- RFs depth stacks indicate difference in d660 behavour between Ethiopia and the southern East African rift (e.g., Boyce & Cottaar, 2021) and suggest that thinnest MTZ resides below Turkana.
- Increased conversion point spread and Fresnel zone width with depth (Fig. 7,10) is accounted for by weighted common conversion point (CCP) stacking following Boyce & Cottaar, (2021) - **see box 5**.

FIGURE 10 (Above): Schematic of receiver function common conversion point (CCP) stacking.

TAKE-HOME MESSAGES

1) New absolute P-wavespeed tomography reveals **discontinuous shallow slow wavespeed structure below East African rift.**
2) New receiver function imaging shows the **thinnest transition zone in East Africa resides below the Turkana Depression.**
3) Evidence for hot upwelling mantle below Turkana suggests **depressed topography** is associated with **Mesozoic-Cenozoic rifting**.
4) **Ethiopian flood basalt volcanism** may be related to the **African plate's position over the thinned present day MTZ in Turkana**.

2 Absolute-Arrival Time Data and Tomographic Resolution

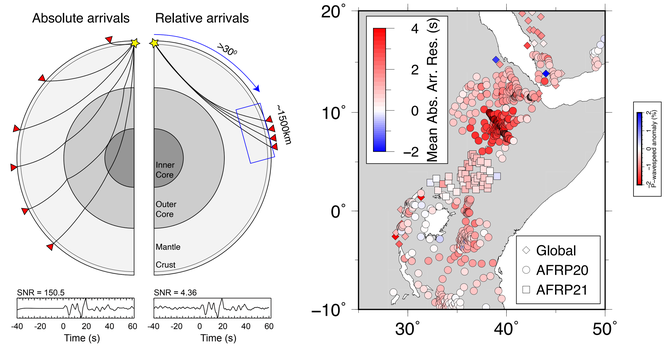

FIGURE 2 (Above left): Schematic of differences between relative and absolute arrival-times. Absolute arrival-times facilitate comparison with the global mean and whole-mantle imaging.
FIGURE 3 (Above middle): Mean P-wave absolute arrival-time residuals for all seismograph networks utilized in this study. Global: Li et al., (2008); AFRP20: Boyce et al., (2021); AFRP21: new data set added here. Residuals are corrected for Earth's ellipticity and station elevation.
FIGURE 4 (Above right): Structural resolution test of input wavespeeds structure **(a,d,g-i)** motivated by previous work (Kounoudis et al., 2021), absolute arrival-time residuals (Fig. 3) and our new tomographic model AFRP21 **(c,f)**. Input anomalies amplitudes are either dV_p= +2.0% or -2.0%. Output models **(b,e,j-l)** are shown on the same color scale. Cross-section locations (X, Y, Z) are shown in **(a)**. Locations of "EHB" stations and temporary deployments are shown as yellow and red triangles **(d)**.

- Absolute Arrival-time Recovery Method (Boyce et al., 2017) applied to data from newly available temporary station deployments to extract ~11,200 direct P-wave and ~1,299 core phase absolute arrival-time residuals facilitating direct comparison to arrival-times from adjacent regions (in contrast to relative arrival-times - see Fig 2).
- Absolute arrival-time residuals in Turkana are less anomalous than below Ethiopia to the north (Fig. 3). Early arrivals occur at the eastern and western extremities of AFRP21 data.
- New data are supplemented with continental and global data sets (Boyce et al., 2021; Li et al., 2008) and are inverted for V_p perturbations w.r.t. ak135 (Kennett et al., 1995) using the global, adaptively parameterized, linearized, least-squares inversion of Li et. al., (2008). Data are corrected for crustal structure prior to inversion using East African seismic constraints (where available) smoothed into Crust1.0 (Laske et al., 2013).
- Resolution of our new model 'AFRP21' in East Africa is sufficient to resolve realistic features, below dense station coverage.
- A narrow E-W fast wavespeed band in Northern Turkana imaged by Kounoudis et al., (2021) and also by AFRP21 is not well recovered in our tests, but is not revealed as an artifact suggesting this is likely a very strong but narrow feature.

5 Receiver Function Stacking Results

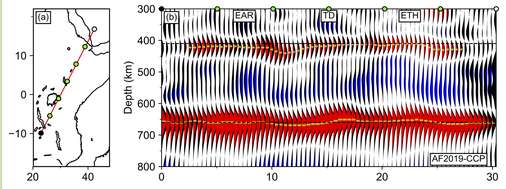

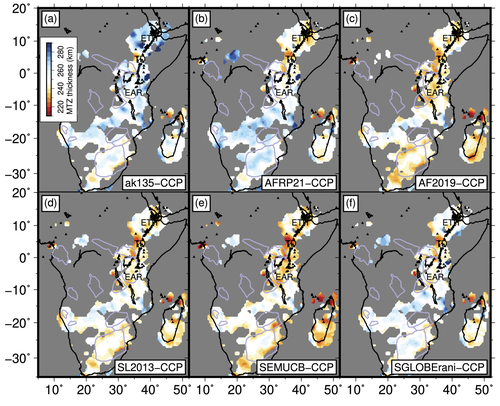

- Delay times of converted S-phases in RFs are mapped to a discontinuity depth using ak135 (Kennett et al., 1995), AFRP21 (Fig. 6), AF2019 (Celli et al., 2020), SL2013SV (Schaeffer & Lebedev, 2013), SEMUCB (French & Romanowicz, 2014) and SGLOBErani (Chang et al., 2015).
- New data facilitates significantly improved CCP stacking below Turkana compared to previous work (e.g., Boyce & Cottaar 2021).
- ak135-CCP is not interpretted because 410km and 660km discontinuity topography is highly correlated impling upper mantle 3D velocity variations are significant (Fig. 12a).
- 3D depth corrected CCP stacks (Fig. 12b-f) show spatial agreement of MTZ thickness in East Africa.
- The thinnest MTZ in East Africa occurs below Turkana, indicating hot upwelling material may be present.

FIGURE 11 (Above left) Waveform cross-sections (along profile in **a**) through AF2019-CCP **(b)** using 0.2Hz maximum frequency. Depths of significant maximum peak amplitude around d410 and d660 depths are highlighted by yellow ticks.
FIGURE 12 (Above right): MTZ thickness within CCP stacks constructed using RF data of maximum frequency 0.2Hz with varying time-to-depth corrections: ak135-CCP **(a)**, AFRP21-CCP **(b)**, AF2019-CCP **(c)**, SL2013-CCP **(d)**, SEMUCB-CCP **(e)**, SGLOBErani-CCP **(f)**. Results are presented only where depths are significant.

Affiliations:
[1]Present Address: Laboratoire de Géologie de Lyon : Terre, Planète, Environnement, Université Claude Bernard, Lyon1, Bâtiment Géode, 2, rue Raphaël Dubois, 69622 Villeurbanne Cedex, France.
[2]Department of Earth Sciences, University of Cambridge, UK. [3]Department of Earth Science & Engineering, Imperial College London, UK. [4]Tulane University, New Orleans, LA, USA.

Funding statement:
This work was supported by the **Natural Environment Research Council** [NERC grant reference number NE/R010862/1], has received funding from the **European Research Council** (ERC) under the European Union's Horizon 2020 research and innovation programme (grant agreement No. 804071 -ZoomDeep) and is supported by the **Centre National de la Recherche Scientifique** at unit UMR5276 (LGL-TPE). I. D. Bastow acknowledges support from **Natural Environment Research Council** grant number NE/S014136/1. C. J. Ebinger acknowledges **National Science Foundation** NSFGEO-NERC award 1824417.

New East African Seismic Networks:

Bastow, I. (2018). Turkana Rift Arrays to Investigate Lithospheric Strains (TRAILS) - UK component. FDSN. doi: 10.7914/SN/SA_2019.
Ebinger, C. (2016). Crust and mantle structure and the expression of extensionin the Turkana Depression of Kenya and Ethiopia. FDSN. doi: 10.7914/SN/Y1_2018.
Nyblade, A. (2017). Broadband seismic experiment in NE Uganda to investigate plume-lithosphere interactions.FDSN. doi: 10.7914/SN/XW_2017.

References:

Boyce, A., et al., (2017), From relative to absolute teleseismic travel-times: the Absolute Arrival-time Recovery Method (AARM), BSSA, 107(5), pp. 2511-2520. *Boyce, A., et al., (2021),* AFRP20: New P-wavespeed model for the African mantle reveals two whole-mantle plumes below East Africa and Neoproterozoic Modification of the Tanzania Craton, Gcubed, 22, e2020GC009302. *Boyce, A., & Cottaar, S. (2021),* Insights into deep mantle thermochemical contributions to African magmatism from converted seismic phases. Gcubed, 22, e2020GC009478. *Celli, N., et al., (2020),* African cratonic lithosphere carved by mantle plumes. Nat. Comms, 11(1), 92. *Chang, S., et al., (2015),* Joint inversion for global isotropic and radially anisotropic mantle structure including crustal thickness perturbations. JGR: Solid Earth, 120(6), pp. 4278-4300. *French, S., & Romanowicz, B. (2014),* Whole-mantle radially anisotropic shear velocity structure from spectral-element waveform tomography. GJI, 199(3), pp. 1303-1327. *Jenkins, J., et al., (2016).* Depressed mantle discontinuities beneath Iceland: Evidence of a garnet controlled 660 km discontinuity? EPSL, 433, pp.159-168. *Kennett, B., et al., (1995),* Constraints on seismic velocities in the earth from traveltimes. GJI, 122, pp. 108-124. *Kounoudis, R. et al., (2021),* Body-Wave Tomographic Imaging of the Turkana Depression: Implications for Rift Development and Plume-Lithosphere Interactions. Gcubed, 22, e2021GC009782. *Laske, G., et al., (2013),* Update on CRUST1.0 : A 1-degree Global Model of Earth's Crust. = Geophys. res. abstracts, 15, abstract egu2013-2658. *Lawrence, J. & Shearer, P. (2006),* Imaging mantle transition zone thickness with SdS - SS finite-frequency sensitivity kernels. GJI, 174(1), pp. 143-158. *Li, C., et. al., (2008),* A new global model for P wave speed variations in Earth's mantle. Gcubed, 9, Q05018. *Ligorria, J. & Ammon, C., (1999),* Iterative deconvolution and receiver-function estimation. BSSA, 89(5), pp.1395-1400. *Merdith, A., et al., (2020),* Extending full-plate tectonic models into deeptime: Linking the neoproterozoic and the phanerozoic, Earth-Sci. Revs, 214, 103477. *Müller, R., et al., (2018),* GPlates: Building a Virtual Earth Through Deep Time. Gcubed, 19(7), pp. 2243-2261. *Schaeffer, A. & Lebedev, S. (2013),* Global shear speed structure of the upper mantle and transition zone. GJI, 194(1), pp. 417-449.

3 AFRP21 Tomographic Model: Relationship to Topography

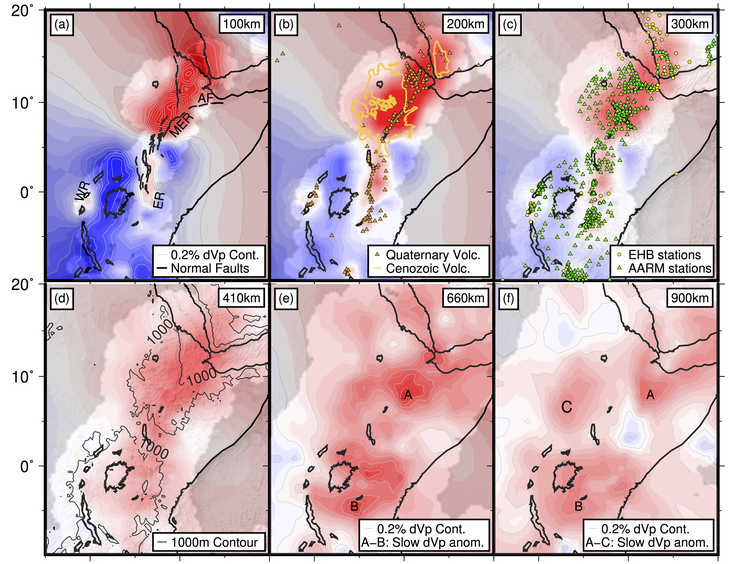

FIGURE 5: AFRP21 African tomographic model at 100-900km depths plotted as percentage deviation from ak135 (dV_p=±1.5%). Only the global data set constrains the gray regions according to the projected ray paths of our temporary seismograph station data. **(a)** 0.2% dV_p wavespeed contours, and normal faults bounding the Neogene-Recent East African rift (black lines). **(b)** Quaternary volcanism (orange triangles) and Cenozoic flood basalt magmatism (yellow outlines). **(c)** "EHB" stations (yellow circles) and temporary deployments (green triangles). **(d)** 1000m surface topographic contour. **(e,f)** 0.2% dV_p wavespeed contours and locations of significant slow wavespeed anomalies referred to in the text (A-C).

- Narrow band of low amplitude fast wavespeeds (dV_p≈0.2% at ~100km depth) separates broad slow wavespeeds below the MER from the narrow slow wavespeed zone below Turkana and ER.
- Slow wavespeeds become continuous at ≥200km depth, but slow wavespeeds are significantly less anomalous in the narrow segment below Turkana and ER (dV_p≈-0.5%) compared to that below MER (dV_p≈-2.0%).
- In all but the very shallow mantle, the relatively subdued topography in the Turkana Depression is underlain by slow wavespeeds.
- The fast wavespeed anomalies to the east and west of Turkana extend southwards below TC at 100km. Fast wavespeed anomalies reduce to (dV_p≤+1.0%) at greater depth.
- At 410km depth, continuous slow wavespeeds of dV_p≤-1.0% extend from the Afar depression to southeastern rift. At 660km distinct slow wavespeeds anomalies (dV_p≤-1.0%) become apparent (A, B), situated below the EP and EAP, respectively. At this depth wavespeeds below Turkana are less anomalous dV_p≤-0.6%.
- Below the MTZ, a third anomaly in (C) emerges but only remains isolated from anomaly B above 1300km depth.

6 Transition Zone Thickness: Relationship to Magmatism

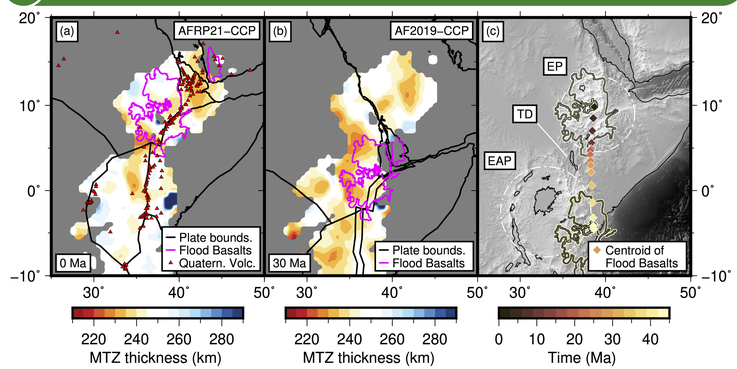

FIGURE 13: East African plate motion above an assumed stationary MTZ. Maps of MTZ thickness (d660 - d410) within AFRP21-CCP **(a)** and AF2019-CCP **(b)** for regions where both d660 and d410 converted arrivals are significant, are fixed to their present day locations. Plate-scale features including coastlines and plate boundaries (black lines), flood basalt magmatism and Quaternary volcanism are plotted at their present day locations **(a)** and reconstructed to 30Ma **(b)**. **(c)** Centroid position of flood basalts (diamonds) shaded by reconstruction time between 0-45Ma plotted over East African topography. The present day outline of flood basalts (white) is reconstructed to 45Ma (beige) for visual reference purposes only. Plate motions reconstructed following Müller et al. (2018); Merdith et al.(2020) using the Paleomagnetic reference frame.

- Present day MTZ is thinned (>15km) below Afar, Turkana and Eastern Rift, but not below Ethiopian flood basalts (Fig. 13a).
- At 30Ma, the Ethiopian flood basalts lay above the thinnest MTZ in East Africa (Fig. 13b).
- Ethiopian flood basalt magmatism was most active at ~30Ma, comtemporaneous with the Eurasian-African collision that caused a significant reduction in northward velocity of Africa. Recently plate motion has increased. (Fig. 13c).
- Assuming a laterally stationary MTZ over ~30Ma (e.g., Lawrence & Shearer, 2008), the main erruptive phase of Ethiopian flood basalt magmatism occured while the African plate slowly moved over a region of substantial mantle upwelling which now lies below Turkana.

alistair.boyce@univ-lyon1.fr / @alistair_boyce